Laser-Induced Decomposition and Ablation Dynamics Studied by Nanosecond Interferometry. 2. A Reactive Nitrocellulose Film

Hiroshi Furutani,[†] Hiroshi Fukumura,*[,†] Hiroshi Masuhara,*[,†] Sigeki Kambara,[‡] Toru Kitaguchi,[‡] Harumichi Tsukada,[‡] and Takeo Ozawa[‡]

Department of Applied Physics, Osaka University, Suita 565, Japan, and Material Science Laboratory, Daicel Chemical Industries, Aboshi-ku, Himeji 671-12, Japan

Received: October 27, 1997; In Final Form: January 28, 1998

Laser-induced decomposition and accompanying ablation dynamics of a reactive nitrocellulose film doped with a Cu-phthalocyanine derivative as a light absorber was investigated by applying a nanosecond interferometric technique. While nitrocellulose does not absorb XeF 351 nm excimer laser pulse, the film is heated instantaneously via rapid photothermal conversion in the doped Cu-phthalocyanine derivative. Below the ablation threshold, the irradiated film expanded transiently with no permanent etching; namely, thermal expansion and contraction processes were directly followed in the ns time region. Above the ablation threshold the expansion of the film was started during the excimer laser pulse, and then explosive decomposition was initiated, continuing in a few hundreds ns after the excitation. Generation of shock wave and ejection of gaseous plume were also observed by nanosecond photographic technique. The shock wave emerged at 100−200 ns after excitation and later than the typical shock wave formation time reported in general. The slow formation is consistent with the slow initiation of the decomposition, suggesting a specific ablation process of the nitrocellulose film. Temperature elevation caused by the excimer laser irradiation results in an exothermic decomposition of nitrocellulose, leading to a further temperature rise of the film. Consequently self-acceleration of the reaction is enhanced and an explosive self-sustaining decomposition is induced after reaching the explosive decomposition condition. Ablation rate was determined to be 0.63 m/s which is slower than that of detonation but faster than that of combustion.

Introduction

Laser ablation has received much attention as unique physicochemical phenomena due to interactions between intense, short optical pulse and materials. As a result of multiphotonic excitation, depletion of the ground state, cyclic multiphoton absorption, and so on, exited states are densely populated in the surface layer, and succeeding processes lead to its morphological changes; laser ablation.[1] It is important and necessary to reveal dynamic behavior of primary and subsequent processes responsible to the morphological changes to gain the knowledge on microscopic mechanism. Since the processes are considered to be induced in a very short period, time-resolved measurements are very useful to interrogate the transient processes of laser ablation.[2] According to this context, many kinds of time-resolved measurements have been carried out, such as picosecond anti-Stokes coherent Raman spectroscopy,[3] time-resolved absorption and emission spectroscopy,[4] time-resolved absorbance measurement at the excitation wavelength,[5] time-resolved optical thermometry,[6] picosecond IR spectroscopy,[7] and time-resolved photography.[8] On the basis of such experimental studies, some transient species and their dynamic processes in laser ablation phenomena have been clarified and considered. For instance, cyclic multiphotonic absorption and photothermal conversion processes are confirmed to be characteristic of high-density excitation of aromatic molecules doped in polymers which is responsible to rapid heat transfer to the surrounding matrix.[9] Ultrafast temperature elevation, leading to pressure jump, chemical reactions, and blast shock wave formation in the irradiated materials have been discussed theoretically and experimentally by Dlott et al.[3a,10−12] The ejection of intact doped molecules was also recently analyzed and considered by us.[13] These microscopic dynamic processes are closely connected with morphological changes, namely, the macroscopic response of irradiated materials. However, little has been known about the dynamics of the macroscopic morphological changes due to the lack of a suitable observation method.

Recently, we developed a new technique to measure rapid and small expansion and contraction occurring during or just after laser excitation with high sensitivity and high temporal resolution. It is nanosecond time-resolved interferometry based on a Michelson interferometer combined with pulsed lasers.[14a] By using the novel method, we have succeeded in showing temporal evolution of macroscopic morphological changes of several different polymer films. In case of PMMA films doped with pyrene or biphenyl as a sensitizer,[14b] expansion of the film prior to the explosive ejection of the ablated fragments was observed during the excimer laser pulse. Even below the ablation threshold, transient expansion of the irradiated PMMA film takes place, although no permanent etching was observed on the irradiated area. It was also shown that the dynamics of the transient expansion varied from polymer to polymer, which was eventually ascribed to the glass transition temperature. Laser-induced decomposition dynamics of a photoreactive triazenopolymer film was quite recently measured and analyzed by the nanosecond interferometry.[15] Triazenopolymer was decomposed directly from solid to gaseous products, and the

[†] Osaka University.
[‡] Daicel Chemical Industries.

S1089-5647(97)03459-7 CCC: $15.00
Published on Web 04/11/1998

CHART 1: Chemical Structures of Nitrocellulose (Right) and Savinyl Blue (Left)

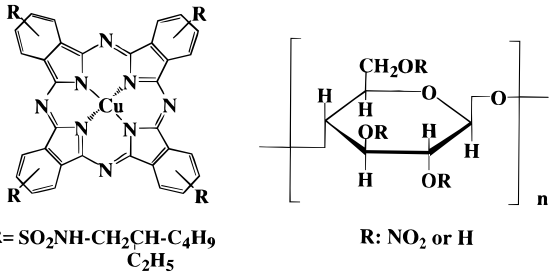

TABLE 1: Content Ratio of Nitrocellulose Sample and Reference Films

	nitrocellulose (NC)	Savinyl Blue (SB)	polyurethane (PU)
NC/SB/PU	30 wt %	25 wt %	45 wt %
SB/PU	0	25	75
NC/PU	30	0	70

etching process was mainly finished during the excitation laser pulse. The decomposition dynamics was dependent on applied fluence, on which we concluded that the decomposition is induced dominantly via a photochemical pathway, and that thermal one also contributes to some extent at a lower fluence near the ablation threshold.

In this article, we examine a reactive nitrocellulose (NC) film and show its novel decomposition dynamics. NC is a highly reactive material and has been widely used as an explosive and propellant. It is well-known that NC is thermally decomposable and releases heat during reaction (exothermic decomposition), namely, its reaction is self-accelerated by the decomposition itself and self-sustained after reaching the explosive decomposition. The chemical nature of NC is different from other polymers, hence NC film is expected to show a specific dynamics of thermal decomposition and macroscopic morphological change upon laser irradiation. Its decomposition dynamics has received much attention in the field of mechanistic study of combustion and burning processes of reactive explosives and energetic propellants. The nanosecond interferometry can directly lighten the solid-to-gas transition process in decomposition, while only conventional analysis has been applied until now.[16] In addition, we have employed nanosecond photography to investigate the gas formation dynamics. On the basis of these measurements, we discuss the decomposition and ablation process of an NC film and its mechanism in detail.

Experimental Section

Materials. The chemical structure of NC (Daicel Chemical Industries) used here is given in Chart 1. Nitrogen content of the NC was about 12.2 wt %, while the highest nitrogen content is 14.15 wt % if all OH groups are completely substituted by ONO_2. A Cu-phthalocyanine with bulky substituents (Savinyl Blue GLS, Sandz, abbreviated as SB) was doped in the sample film as a light absorber. The chemical structure is also shown in Chart 1. In addition, polyurethane (PU) was added as a binder to form a stable film. Mixture of NC, SB, and PU were dissolved in methyl ethyl ketone with the appropriate wt %, and from the solution films were prepared by a bar-coating method and dried for 2 min at 110 °C in air to remove the residual solvent. The thickness of the film was ca. 1 μm. The content of the three components, NC, SB, and PU, of the prepared films is listed in Table 1. Other reference films of NC/PU and SB/PU were also prepared similarly. Absorption spectra of NC/SB/PU (sample) film and the NC/PU (reference) films are shown in Figure 1. Appreciable absorption of the NC/SB/PU film at the excitation wavelength (351 nm) is clearly ascribed to SB, which will sensitize the ablation of the sample film.

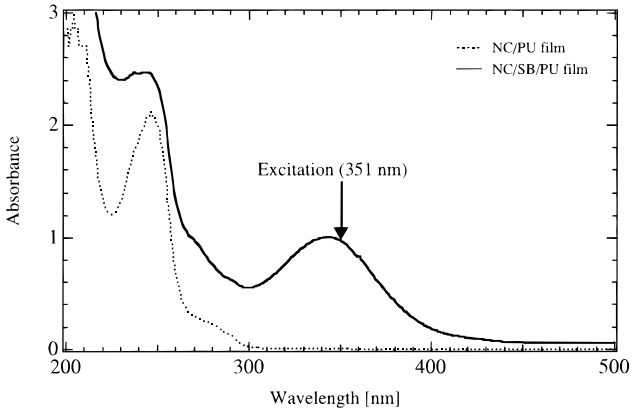

Figure 1. Absorption spectra of nitrocellulose sample and reference films. For abbreviations, see Table 1.

Ablation Experiment. A XeF excimer laser (Lambda Physik Lextra 200, 351 nm, 30 ns fwhm) was used as an excitation pulse for inducing decomposition and ablation. The fluence was adjusted with partially transmitting laser mirrors. A central area of the excimer laser pattern with a homogeneous intensity distribution was chosen with an appropriate aperture and then focused onto the sample surface by using a quartz lens (f = 250 mm). Fresh surface of the sample film was used in every measurement. Laser intensity was monitored by a joulemeter (Gentec, ED-200) with an oscilloscope (Hewlett-Packard, HP54522A). Etch depth was measured by a surface depth profiler (Sloan, Dektak^2). All experiments were done in air at room temperature.

Nanosecond Interferometry. The nanosecond interferometry applied here is the same as reported before.[14] Briefly, the second harmonic of a Q-switched Nd^{3+}:YAG laser (Continuum Surelite I, 532 nm, 10 ns fwhm) was used as a probe light source of the interferometer to measure the excimer laser-induced morphological change of the present films. Interference patterns were captured by a CCD camera (Sony, XC77, 512 × 512 pixels) and then analyzed. Time-resolved measurement was carried out by controlling the delay time (Δt) between excitation and probe laser pulses with a digital delay/pulse generator (Stanford Research System, DG 535). Here we define $\Delta t = 0$ when the peaks of both laser pulses are overlapped completely.

The optical configuration to avoid the disturbance of ejected fragments of gaseous products is applied, where the surface of the quartz substrate, facing to the polymer film, and the back surface of the quartz plate are almost in parallel. The reflected light from the latter surface interferes with the reflected one from the polymer surface, generating interference fringe patterns. The shift of interference fringes in the irradiated area is ascribed to the change of thickness and/or refractive index of the polymer film. Practically it is considered that the latter change is minor.

It should be noted that all the interference fringe patterns are not identical to each other, since interference images were acquired for different positions for interrogating fresh surface and optical condition changed from shot to shot. In the experiment a movement of the fringe to the right side represents an etching of the polymer film, which was attained by adjusting the optical condition. As a shift of one fringe spacing to the right corresponds to an etching of 266 nm, a half-wavelength of probe laser, expansion and etching behavior can be elucidated

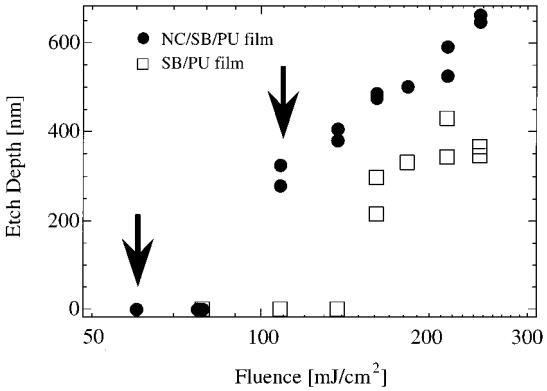

Figure 2. Etch profile of nitrocellulose and reference films excited with 351 nm excimer laser irradiation. Arrows represent the laser fluence at which experiments were conducted.

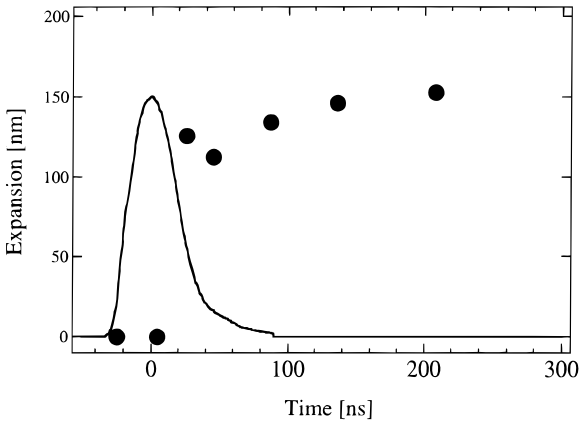

Figure 3. Nanosecond expansion behavior of the NC/SB/PU film at 60 mJ/cm^2. Solid curve represents an excimer laser pulse.

by analyzing interference patterns at each delay time with the resolution of a few tens of nm.

Nanosecond Photography. Details of the nanosecond photography is described elsewhere.[8c] An irradiation light source is the same excimer laser as described above, and fluorescence of R6G solution excited by the second harmonic of Nd^{3+}:YAG laser was used as nanosecond flash back-illumination (duration ~20 ns) for the imaging of ejected fragments and products with size of ca. 10 μm. Imaging and time-controlling devices were the same as those used in the nanosecond interferomety.

Results and Discussion

Nanosecond Heating of Polymer Matrix Due to Rapid Photothermal Conversion by Savinyl Blue. As NC does not absorb 351 nm laser light, SB is responsible to laser light absorption and works as a sensitizer for laser ablation. Namely, SB is an efficient molecular heater upon excimer laser irradiation, and actually in pure amorphous film of SB temperature at the surface layer was estimated to be 1500 °K when excited at 55 mJ/cm^2.[17] It is considered that a number of photons could be absorbed during the excitation pulse without appreciable saturation. Under high-intensity excitation, densely formed excited states undergo mutual annihilation leading to recovery of the ground state. Thus SB molecules can absorb photons repeatedly during the excitation pulse. Competitively the excited states also absorb photons, and the higher excited states are formed and relax to the original excited states. As the duration of nanosecond excitation pulse is much longer than the recovery time of the excited states, the cyclic absorption by the excited states is probable and the surrounding matrix should be heated.[9] Indeed, it was observed that a hot band of the ground state of SB was generated upon ultrafast laser irradiation, meaning the temperature elevation.[18]

Etch Depth. Fluence dependence of etch depth of both NC/SB/PU and SB/PU is given in Figure 2, where the ablation threshold was determined to be about 80 and 140 mJ/cm^2, respectively. Since the absorbance of both films is same, it is obvious that NC lowers the ablation threshold, which is of course considered to be due to reaction of NC. To avoid a contribution of PU ablation, we chose 110 mJ/cm^2 for time-resolved interferometric and photographic measurements, as the ablation of SB/PU film is impossible at this fluence. We also conducted similar measurements at 60 mJ/cm^2, below the ablation threshold.

Expansion Dynamics below the Ablation Threshold. At a fluence of 60 mJ/cm^2, below the ablation threshold, nothing was observed for NC/SB/PU film by nanosecond photography. This means fragments as large as ~10 μm are not generated appreciably. On the other hand, a small transient morphological change induced by the excimer laser irradiation was observed by nanosecond interferometry which was analyzed and shown in Figure 3. The irradiated film began to expand at the late stage of the excimer laser pulse and reached a height of about 150 nm at the delay time (Δt) = +120 ns. The expansion disappeared completely after enough delay time, namely, no permanent etching of the film was left at this fluence. As explained above, the transient expansion is considered to be a thermal one which is due to heating of the NC/SB/PU film via rapid photothermal conversion of SB. In addition it is may be considered that thermal decomposition of reactive NC takes place during the excimer laser irradiation and the formed gas molecules induce the transient expansion. However, any cracking, hole, and protrusion, suggesting gas formation, were not obtained by observing surface morphology. The decomposition reaction of NC is an exothermic thermal reaction as mentioned before, while the expanding behavior stopped almost at the end of the excimer laser pulse. This means that the condition under which the decomposition is self-sustained and self-accelerated was not realized at 60 mJ/cm^2.

Shock Wave Propagation and Plume Ejection above the Ablation Threshold. Nanosecond photography at a fluence of 110 mJ/cm^2, above the threshold, reveals explosive ejection of ablated products and shock wave propagation as shown in Figure 4. Generation of the fast shock wave was detected at $\Delta t \sim +200$ ns, which was followed by a slow plume ejection. Ejected products were observed as dark shadow in Figure 4g,h, while no large debris or fragment such as those reported for doped PMMA films could be seen.[4b−d] This suggests that the NC/SB/PU film was efficiently decomposed to molecular fragments smaller than the wavelength.

In Figure 5, time evolution of the shock wave propagation and plume ejection were given. The velocity of the former propagation was about 160 m/s, which is not so different from that observed in the ablation of PMMA,[4b] poly(ethylene terephthalate) (PET),[8b] and triazenopolymer films.[15] The velocity of the plume ejection (~64 m/s) is also comparable to that of these polymer films. It is worth noting that the shock wave appeared abruptly at later stages than 100 ns, which is different compared to the above three polymer films. In the latter cases the shock wave became visible from +10 to 100 ns. The present characteristic etching behavior of the NC/SB/PU film upon laser irradiation is believed to come from peculiar chemical decomposition dynamics of NC.

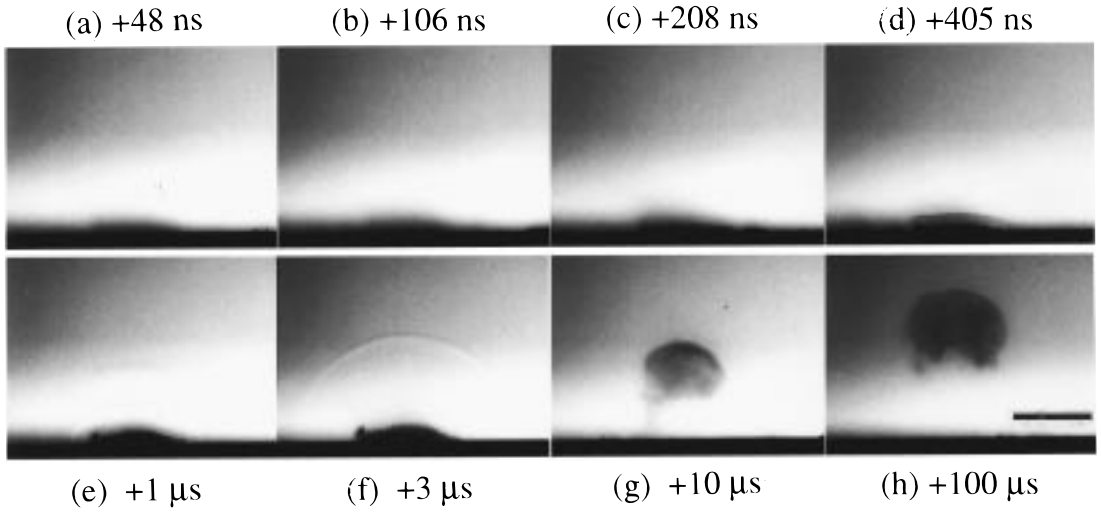

Figure 4. Nanosecond photographic images of the NC/SB/PU film at 110 mJ/cm^2. The bar in the figure represents 1 mm.

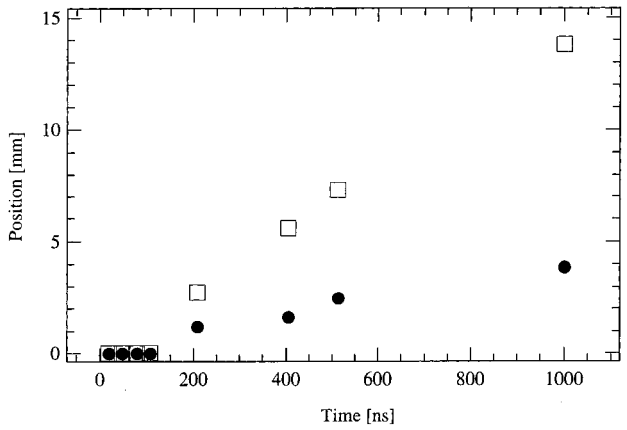

Figure 5. Propagation behavior of shock wave (□) and fragments (●) from the NC/SB/PU film upon excitation of 110 mJ/cm^2.

Ablation Dynamics above the Threshold. Figure 6A shows a series of time-resolved interference images at a fluence of 110 mJ/cm^2 above the threshold. In this measurement, optical conditions were adjusted so that a movement of the fringe to the left represents an expansion of the irradiated NC/SB/PU film. The whole area of the excimer laser pulse, which has a spatially inhomogeneous profile, was applied to the film surface, and the morphological dynamics of ablated area (denoted as center) was compared with that of nonablated outside area (denoted as border). The small drawings inserted above and below the images are the schematic profiles of induced morphological changes which were analyzed from the deformation of the fringe patterns.

Figure 6A(a) shows an interference pattern at $-\infty$ ns, before excimer laser irradiation. Except for the small area on the right side with complex pattern, the fringe pattern consists of straight lines without deformation, representing a smooth flat surface. The complex fringe area which is also seen in some other interference images at different delay times (e.g. at the bottom of Figure 6A(f)) is an edge area of the target film and has no meaning in the present results. At +8 ns fringes in both center and border were slightly deformed to the left side, which represents an expansion of the irradiated NC/SB/PU film. It is noticed that darkening of the irradiated film surface was also observed. With increasing of delay time, deformation of the fringe to the left side became larger, and stopped around +50 ns, meaning termination of expansion of the irradiated area. Later from this delay time, center and border areas began to show different morphological behavior. In the range from +200 ns to +1 μs (Figure 6A(d−f)), the fringe in the border did not change, while that in the center moved to the right side abruptly, indicating a fast decrease of film thickness. The latter fringe movement finished at +1 μs and then gradually approached to final interference pattern. At +100 μs the temporal change of fringe pattern ceased completely, which corresponds to the final etch pit. From the deformation of the fringe patterns, precise analysis of induced morphological change was performed, and the dynamics will be discussed later.

It is also worth noting that fringe patterns were visible at all delay times in the ablation of the NC/SB/PU film. This result is contrary to the ablation of doped PMMA films where the fringe became invisible after +50 ns due to the ejection of ablated debris or fragments.[14] Thus, it is concluded that no large debris or fragment of wavelength order was ejected upon laser ablation, which is consistent with the results revealed by the nanosecond photography.

One of the advantages of image measurement by the nanosecond interferometry is that the respective morphological dynamics in different areas of the film can be analyzed simultaneously. Since the border area has lower fluence than that of the center area as shown schematically in Figure 6B, the former area was not ablated, which is a good reference for analyzing etching behavior. Expansion and contraction dynamics of Figure 6A was analyzed and plotted against delay time in Figure 7. Expansion in both center and border areas was initiated during the excimer laser pulse and continued until +50 ns. The expanding behavior in both areas was almost similar to each other, but the absolute displacement was different because of the inhomogeneous fluence distribution. After +50 ns, the increase of the film thickness in the center area was stopped and followed by the decrease, although the expansion in the border area was still persistent. Then the latter the border area showed the slow decrease in the s time range and came back to the original value (zero displacement), namely, no permanent etching being observed. The behavior of the border area, irradiated below the ablation threshold, can be interpreted well as expansion and the following contraction dynamics. On the other hand, in the center area a monotonic decrease continued at least till +500 ns, and then a further slow decrease was observed in the μs time range. As the behavior of the center area is different from that of the border area in +50 ns ∼+500 ns region and the permanent etching was observed, it is considered that ablation (etching) takes place in the time range.

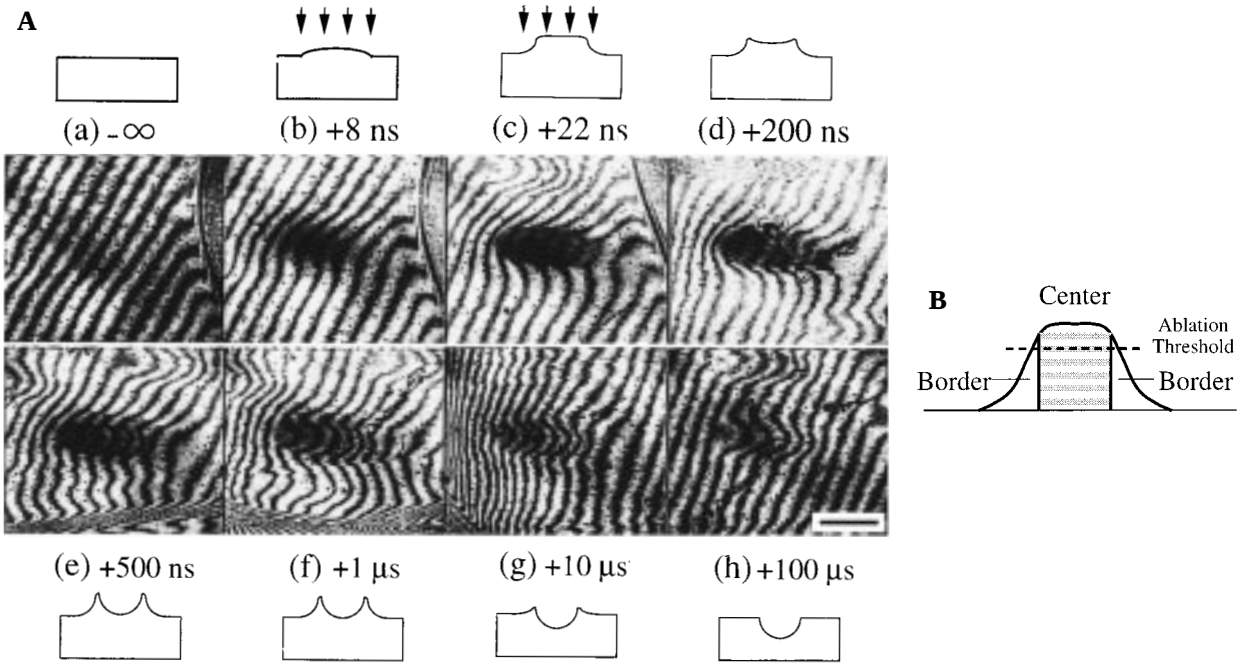

Figure 6. (A) Nanosecond interferometric images of the NC/SB/PU film at 110 mJ/cm^2. The bar in the figure represents 1 mm. Schematic illustration of expansion and etching at each stage is given above or below the images. (B) Excimer laser profile and definition of center and border.

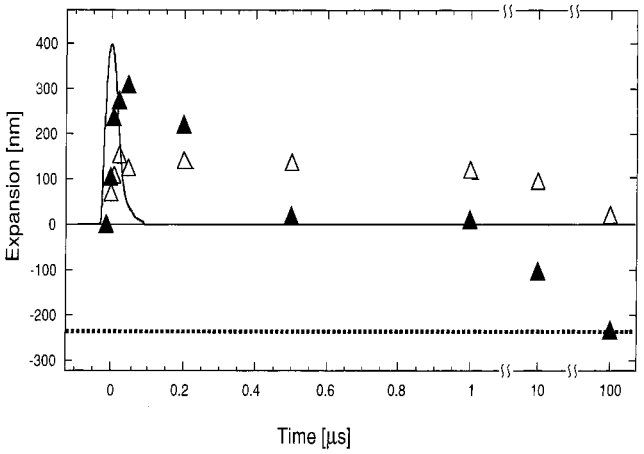

Figure 7. Expansion/contraction and ablation dynamics of the NC/SB/PU film at 110 mJ/cm^2. The examined area is center (▲) and border (△). Dotted line represents the etch depth measured by a depth profiler.

The decrease of the central part in the few tens of μs region is due to the thermal contraction owing to the slow heat dissipation, as similar behavior was observed for both central and border parts.

It is worth noting that the delayed initiation of ablation (etching) process is characteristic of the present film, as etching of triazenopolymer[15] and doped PMMA films[14] started during the excitation pulse. As mentioned above, the slow initiation is consistent with its slow emerging of the shock wave observed by the nanosecond photography.

Finally, it is pointed out that the temperature elevation does not involve phase transition. Dynamics at the initial expanding stage ($\Delta t < +100$) was common to both center and border areas, and maximum expansion observed at +100 ns with a fluence of 110 and 60 mJ/cm^2 was about 300 and 150 nm, respectively. The maximum expansion almost linearly depends on applied fluence, which was confirmed precisely for poly(methyl acrylate) (PMA) film doped with pyrene.[14b] The linear dependence of laser-induced thermal expansion of PMA film suggested that the thermal property is not changed so much in the examined fluence region. Namely, glass−rubber transition is not involved. Actually, PU is already rubber at room temperature and Tg of NC is about 313 K[19] which is close to the room temperature. Therefore, laser-induced temperature jump (higher than 300 K) as done here, did not induce such transition and provided the linear expansion.

Decomposition and Ablation Mechanism. It is quite interesting that the decomposition of the NC film started from ∼+50 ns, not during the excimer laser. The initial thermal expansion of the NC/SB/PU film is quite indicative that the decomposition is a thermal process. If no further heat energy is supplied to the film after the excimer laser irradiation, the temperature of the NC film will decrease owing to the heat dissipation and thermal reactions during the excitation laser pulse will come to the end. However, it has been shown that exothermic and explosive decomposition of NC occurs above an ignition temperature of about 450 K.[20] Since the surface temperature of the NC/SB/PU film was estimated to be about 1400−1800 K on the basis of the simple Lambert−Beer law, the exothermic decomposition could be induced and sustain the thermal decomposition itself. But there is still a remaining question; what was abruptly initiated from +50 ns. In the conventional heating experiment, it is known that NC undergoes combustion after the decomposition, which is because the exothermic decomposition elevates the temperature, accelerates the decomposition itself, and finally combustion condition can be attained. Therefore, it is expected in the present laser experiment that the combustion condition of NC be first attained at +50 ns and end at +500 ns.

Combustion processes and conditions for mixtures of NC and nitroglycerin (NG) have been well investigated as typical propellants,[21] which is helpful to discuss the present dynamics. In Table 2, combustion condition of the mixture is given as a reference. It is well accepted that Chart 2 is a model of combustion of solids where burning reaction zones, such as burning surface, burning gas, and solid are included. Temperature at the reaction surface may reach 1400−1800 K by reaction of combustible gas produced via decomposition at the burning surface. It is also known that combustion starts after

TABLE 2: Combustion Condition of Solid Mixture of Nitrocellulose and Nitroglycerin (Taken from Ref 22)[a]

T_s	600−700 K
T_g	1400−1500 K
σ	$(2-4) \times 10^{-3}$ nm/ns

[a] T_f, temperature at burning solid surface; T_g, temperature at burning reaction zone; σ, burning rate.

CHART 2: Illustration for Combustion of Materials: Solid Surface Is Decomposed and Vaporized, and the Surface Draws Back

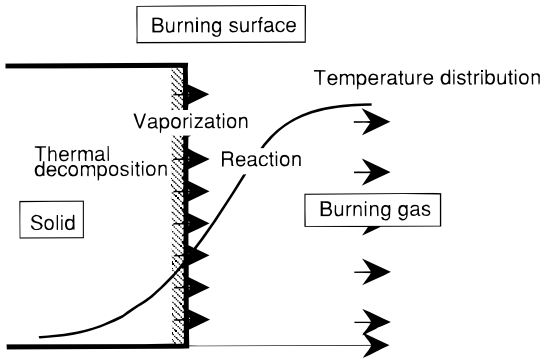

a certain delay even under conventional heating. The delay time is of course dependent on temperature and considered to be necessary for attaining the combustion condition. In the present case, although excimer laser irradiation would rapidly heat the irradiated surface of the NC/SB/PU film up to 1400−1800 K, decomposition of NC to combustible gas molecules and their evaporation should take some time. After the evaporation, chemical reactions also would occur to attain the combustion temperature. All these processes should be responsible for the delayed initiation of ablation.

The existence of such a precombustion process may be consistent with the darkening of irradiated film surface. The darkening appeared from +8 ns as shown in Figure 6A, which is quite early compared to the etching of the film, and continued to late stages after 1 μs. In general the surface darkening is considered to be due to ejection of small ablated fragments and gaseous products or to refractive index change of the film by decomposition products. Thus, we consider that decomposition and following gas evaporation at the surface layer may start immediately and that the decomposed products should be cleared up around 1 μs.

The measured decomposition rate of the present film was about 6.3×10^{-1} m/s and is quite larger than that in ordinary combustion of NC/NG composite (Table 2) or glycerin azido polymer ($\sim 10^{-2}$ m/s).[23] Laser-induced decomposition of the NC/SB/PU film can be attributed to an explosive combustion because of the higher decomposition rate. The large difference of decomposition rate seems to come from the rapid appearance of the combustion condition by excimer laser irradiation which can never be attained by the other conventional heating method. In the present case, the surface temperature of 1400−1800 K is estimated, while the initial temperature in ordinary combustion is less than 400 K.[20] Furthermore, it was reported that rapid pressure jump ($\sim$1 GPa) occurred upon laser ablation,[24] which also may accelerate the decomposition (burning) rate. It is well-known that an increase of initial temperature and pressure causes an increase in burning rate, which of course accelerates decomposition and following evaporation of decomposed gaseous products in solid phase. Thus, these extreme conditions characteristic of excimer laser irradiation lead to the present unique decomposition and ablation dynamics.

Summary

The morphological dynamics of a reactive NC film doped with phthalocyanine derivative as a light absorber upon excimer laser irradiation above and below the ablation threshold has been revealed by applying nanosecond time-resolved interferometry and photography. On the basis of the revealed morphological dynamics and physiochemical properties of nitrocellulose, the time-dependent morphological change was discussed and its mechanism was considered.

Below the ablation threshold, although no etching of irradiated film surface occurred, transient expansion and the following contraction were observed, which is ascribed to thermal heating via rapid photothermal conversion process of doped phthalocyanine derivative. Above the ablation threshold, the irradiated film first underwent expansion, and then decomposition of the film started abruptly at 100 ns after excitation. An exothermic decomposition of the NC/SB/PU film, initiated by the excimer laser irradiation, elevated its temperature and accelerated the decomposition itself. Then after +100 ns, the combustion condition was finally attained and explosive combustion was started abruptly and continued until +500 ns, giving shock wave and gaseous plume ejection. The much longer decomposition (burning) rate than that of ordinary combustion can be ascribed to the extreme conditions such as high pressure and temperature. It is noticeable that the rapid heating by the excimer laser irradiation makes it possible to reveal dynamic aspects of solid decomposition.

Acknowledgment. This work was partially supported by Grants-in-aid from the Ministry of Education, Science, Sports, and Culture of Japan (07554063, 06239101). SB was kindly supplied by Mitsui Toatsu Chemicals, Inc.

References and Notes

(1) (a) Srinivasan, R.; Braren, B. *Chem. Rev.* **1989**, *89*, 1303. (b) Bäuerle, D. *Laser Processing and Chemistry*; Springer-Verlag: Berlin, 1996. (c) Duley, W. W. *UV Lasers: Effects and Applications in Materials Science*; Cambridge University Press: Cambridge, 1996.

(2) (a) Koren, G.; Yeh, J. T. C. *J. Appl. Phys.* **1984**, *56*, 2120. (b) Dyer, P. E.; Sidhu, J. *J. Appl. Phys.* **1988**, *64*, 4657. (c) Masuhara, H.; Itaya, A.; Fukumura, H. In *Polymers in Microlithography*; Reichmanis, E., MacDonald, S. A., Iwayanagi, T., Eds.; American Chemical Society: Washington, DC, 1989.

(3) (a) Hare, D. E.; Dlott, D. D. *Appl. Phys. Lett.* **1994**, *64*, 715. (b) Hare, D. E.; Franken, J.; Dlott, D. D. *J. Appl. Phys.* **1995**, *77*, 5950.

(4) (a) Arnold, B. A.; Scaiano, J. C. *Macromolecules* **1992**, *25*, 1582. (b) Fukumura, H.; Takahashi, E.; Masuhara, H. *J. Phys. Chem.* **1995**, *99*, 750. (c) Fujiwara, H.; Nakajima, Y.; Fukumura, H.; Masuhara, H. *J. Phys. Chem.* **1995**, *99*, 11481. (d) Fujiwara, H.; Fukumura, H.; Masuhara, H.; *J. Phys. Chem.* **1995**, *99*, 11844.

(5) (a) Davis, G. M.; Gower, M. C. *J. Appl. Phys.* **1987**, *61*, 2090. (b) Frisoli, J. K.; Hefetz, Y.; Deutsch, T. F. *Appl. Phys.* **1991**, *B52*, 168. (c) Fujiwara, H.; Hayashi, T.; Fukumura, H.; Masuhara, H. *Appl. Phys. Lett.* **1994**, *64*, 2451.

(6) (a) Wen, X.; Tolbert, W. A.; Dlott, D. D. *Chem. Phys. Lett.* **1992**, *192*, 315. (b) Lee, I.-Y. S.; Wen, X.; Tolbert, W. A.; Dlott, D. D. *J. Appl. Phys.* **1992**, *72*, 2440.

(7) Lippert, T.; Koskela, A.; Stoutland, P. O. *J. Am. Chem. Soc.* **1996**, *118*, 1551.

(8) (a) Srinivasan, R.; Braren, B.; Casey, K. G.; Yeh, M. *Appl. Phys. Lett.* **1989**, *55*, 2790. (b) Srinivasan, R.; Casey, K. G.; Braren, B.; Yeh, M. *J. Appl. Phys.* **1990**, *67*, 1604. (c) Tsuboi, Y.; Fukumura, H.; Masuhara, H. *Appl. Phys. Lett.* **1994**, *64*, 2745.

(9) Fukumura, H.; Masuhara, H. *Chem. Phys. Lett.* **1994**, *221*, 373.

(10) Dlott, D. D. *J. Opt. Soc. Am. B* **1990**, *7*, 1638.

(11) (a) Dlott, D. D.; Fayer, M. D. *J. Chem. Phys.* **1990**, *92*, 3798. (b) Chen, S.; Lee, I.-Y. S.; Tolbert, W. A.; Wen, X.; Dlott, D. D. *J. Phys. Chem.* **1992**, *96*, 7178.

(12) Tokmakoff, A.; Fayer, M. D.; Dlott, D. D. *J. Phys. Chem.* **1993**, *97*, 1901.

(13) Fukumura, H.; Mibuka, N.; Eura, S.; Masuhara, H.; Nishi, N. *J. Phys. Chem.* **1993**, *97*, 13761.

(14) (a) Furutani, H.; Fukumura, H.; Masuhara, H. *Appl. Phys. Lett.* **1994**, *65*, 3413. (b) Furutani, H.; Fukumura, H.; Masuhara, H. *J. Phys. Chem.* **1996**, *100*, 6871.

(15) Furutani, H.; Fukumura, H.; Masuhara, H.; Lippert, T.; Yabe, A. *J. Phys. Chem. A* **1997**, *101*, 5742 (1st paper of the series).

(16) Kosoridis, C. E.; Skordonlis, C. D. *Appl. Phys. A* **1993**, *56*, 64.

(17) Hosoda, M.; Furutani, H.; Fukumura, H.; Masuhara, H.; Nishii, M.; Ichinose, N.; Kawanishi, S. *Rev. Laser Eng.* **1997**, *25*, 306 (in Japanese).

(18) Ichikawa, M.; Fukumura, H.; Masuhara, H.; Koide, A.; Hyakutake, H. *Chem. Phys. Lett.* **1995**, *232*, 346.

(19) *Kobunshi Zairyo Binran*; Corona Pub.: Tokyo, 1973 (in Japanese).

(20) Urbanski, T. *Chemistry and Technology of Explosives*; Pergamon Press: Oxford, 1965; Vol. 2.

(21) Williams, F. A. *Combustion Theory: The Fundamental Theory of Chemically Reacting Flow System, 2nd ed.*; Bengiamin/Cummings Pub.: Menlo Park, CA, 1985.

(22) Kubota, N.; Ishihara, A. *Proceedings of the 20th Symposium (International) on Combustion*, 1984; p 2035.

(23) Ben-Eliahn, Y.; Haas, Y.; Welner, S. *J. Phys. Chem.* **1995**, *97*, 6010.

(24) Bennett, L. S.; Lippert, T.; Furutani, H.; Fukumura, H.; Masuhara, H. *Appl. Phys. A* **1996**, *63*, 627.